Scientific Research Report

HDAC5-Mediated Acetylation of p100 Suppresses Its Processing

Jianqi Wang *, *Shuainan Wu*, *Lu Liu*, *Ying Pang*, *Zhaobao Li*, *Hong Mu*

Department of Stomatology Clinic, Cangzhou Central Hospital, Cangzhou, Hebei, China

ARTICLE INFO

Article history:
Received 5 July 2022
Received in revised form
7 August 2022
Accepted 16 August 2022
Available online 23 September 2022

Key words:
HDAC5
Inflammation
Inhibition
Periodontitis

ABSTRACT

Introduction: Periodontitis is a condition involving chronic inflammation in the gums, periodontal ligaments, cementum, and alveolar bone. Nuclear factor-κB (NF-κB) activation is the prominent mediator of inflammation and osteoclast differentiation. The role of histone deacetylase 5 (HDAC5) in periodontitis development and NF-κB regulation is not fully understood.

Methods: We used primary mouse bone marrow–derived osteoclast cultures in vitro and a mouse model of chronic periodontists (CPD) treated with the HDAC4/5 inhibitor LMK-235. Real-time polymerase chain reaction, micro computed tomography, flow cytometry, western blot, and immunoprecipitation were used to study proinflammatory cytokines, NF-κB activation, HDAC5 activity, and the interaction of HDAC5 with NF-κB p100.

Results: LMK-235, a selective inhibitor of HDAC4 and HDAC5, reduced osteoclast marker gene expression (*Cstk*, *Acp5*, and *Calcr*) and tartrate-resistant acid phosphatase activity in primary osteoclast cultures. LMK-235 reduced the increase in cementoenamel junction–alveolar bone crest distance, inflammatory cell infiltration of gingival tissues, and expression levels of interleukin (IL)-1β, tumor necrosis factor alpha, IL-6, and IL-23a, indicating an ameliorative effect on CPD. Immunoprecipitation experiments have further confirmed p100–HDAC5 interaction, acetylation levels of p100, and NF-κB activation.

Conclusions: These results indicate that HDAC5 binds and deacetylates p100, leading to its activation, increased proinflammatory cytokine production, gingival infiltration, and osteoclast differentiation, thus promoting alveolar bone resorption. HDAC5 inhibition is therefore a potentially promising therapeutic strategy for the treatment of periodontitis.

Introduction

Periodontitis (PD) is a chronic inflammatory condition mediated by the bacterial flora of the oral cavity. It may affect all parts of the tooth, including gums, periodontal ligaments, cementum, and alveolar bone.[1,2] Bone destruction resulting from osteoclast activation in advanced PD eventually results in tooth loss.[3,4] Inflammatory cytokines such as interleukin (IL)-1β, IL-6, and tumor necrosis factor alpha (TNF-α) facilitate the gingival tissue infiltration with the CD45-/CD11b-positive myeloid cells.[5,6] Osteoclast differentiation from monocytes/macrophage precursors is positively regulated by macrophages, colony-stimulating factor (CSF)-1, IL-23a, and the secretion of receptor activator for nuclear factor-κB (NF-κB) ligand (RANKL) that interact with osteoclast receptor activator for NF-κB (RANK).[7]

Distinct from predominantly proinflammatory canonical NF-κB activation that is based on IκBα, RelA, and NF-κB p50 complex formation and p50 subunit nuclear translocation, transcription factors activated in the noncanonical NF-κB pathway p52/RelB NF-κB complex depend on their precursor nuclear factor NF-κB p100 subunit (p100), the precursor and feedback inhibitor of p52 and RelB.[8] RANKL-RNAK ligation activated NF-κB–inducing kinase (NIK), which phosphorylates IκB kinase-α, triggering p100 phosphorylation and processing.[9,10] RANKL-RANK–activated noncanonical NF-κB p100/p52 is the essential pathway in osteoclastogenic bone disease.[11] Regulators of this pathway have therapeutic potential for inflammation-related bone disease, including periodontic diseases.[12]

Histone deacetylases (HDACs) play a crucial role in gene expression regulation by modifying chromosome structural

* *Corresponding author*. Department of Stomatology Clinic, Cangzhou Central Hospital, No. 16 Xinhua West Road, Cangzhou, 061000, Hebei, China.
E-mail address: wangjianqi0612@163.com (J. Wang).

https://doi.org/10.1016/j.identj.2022.08.007

modification through histone deacetylation. HDAC has also been shown to regulate protein function through direct binding and interaction.[13] LMK-235 is a potent, selective inhibitor of HDAC4/5.[14] Inhibition of HDACs was demonstrated to reduce NF-κB p65 activation in vitro.[15] In this study, we explore the effect of LMK-235 on p100 deacetylation and its effect on PD and osteoclast differentiation.

Materials and methods

Animal housing

All animal experiments were approved by the ethics committee of Cangzhou Central Hospital and performed following the *National Institute of Health Guide for the Care and Use of Laboratory Animals*. Wild-type (WT) mice on C57BL/6 background at 8 weeks old were purchased from Cyagen Biosciences Inc. B6N.129-Map3k14 tm1Rds /J (NIK$^{-/-}$) mice (025557) on B6/129 background at 8 weeks old were purchased from the Jackson Laboratory.

Cell cultures

CSF-1 conditioned media
LADMAC (ATCC) was used as a source of CSF-1 for bone marrow macrophage differentiation. LADMAC cell–conditioned media (LCM) was produced as reported previously.[16]

Primary osteoclast cultures
The tibial bones were carefully dissected from the WT and NIK$^{-/-}$ mice. Bone marrow cells were flushed from femurs and tibia of age-matched mice (6–8 weeks) by perfusion with 2 mL of phosphate buffer saline (PBS, Gibco). The resulting cell suspension was further dissociated by pipetting and centrifuged at 300 g. Bone marrow–derived macrophages were differentiated by culturing bone marrow cells in Dulbecco's Modified Eagle Medium (DMEM) supplemented with 20% fetal bovine serum and 30% LCM for 4 to 6 days. Osteoclast differentiation was induced by culturing bone marrow–derived macrophages in LCM supplemented with mouse RANKL (Thermo Fisher Scientific; 50 ng/mL) for 4 days.

Cell treatment

Primary osteoclast culture cells were treated with LMK-235 (5, 10, and 20 nM; SelectChem) by adding LMK-235 to RANKL differentiation media. Dimethyl sulfoxide (DMSO) was used as a control. Primary osteoclast cultures were pretreated with LMK-235 (20 nM) for 2 hours and then stimulated with lipopolysaccharide (LPS; *Escherichia coli* 055:B5; Sigma-Aldrich) 1 μg/mL for 6 and 24 hours or Pam3csk4 (tlrl-pms; InvivoGen) for 6 hours.

RNA isolation and quantitative real-time polymerase chain reaction

The total RNA was extracted using an RNeasy Plus Mini Kit (Qiagen) according to the kit protocol. The RNA was reverse-transcribed to complementary DNA (cDNA) using Maxima H Minus cDNA Synthesis Master Mix with double-strand–specific DNase (dsDNase; Thermo Fisher Scientific). Gene expression was detected using Power SYBR Green Master Mix (Thermo Fisher Scientific) with the mouse-specific primers using 10 ng of the initial cDNA template. Amplicons were detected by QuantStudio 3 real-time polymerase chain reaction (RT-PCR; Applied Biosystems). Cycle-threshold values of the target genes were normalised to GAPDH, and the fold change was calculated using the ($2^{-\Delta\Delta CT}$) method.

Tartrate-resistant acid phosphatase (TRAP) assay

An Acid Phosphatase Assay Kit (Abcam) detected TRAP activity. Briefly, cells were washed with PBS and lysed in citrate buffer + 0.1% Triton X-100 for 5 minutes of incubation at room temperature. The lysates were transferred to 96 well plates. Then 100 μL p-nitrophenyl phosphate and disodium salt were added to the wells. After another 5 minutes of incubation, the reaction was stopped by adding 50 μL 0.5 M NaOH. The optical density (OD) was detected at a 405-nm absorption peak using an 800 TS Absorbance Reader (BioTek Instruments). The OD in DMSO treated control was considered as 100% osteoclastogenesis.

Chronic periodontitis model

The mice were anaesthetised with ketamine hydrochloride (100 mg/kg body weight) and xylazine (4 mg/kg body weight). Subgingival tissues of first and second molars (M1 and M2) were ligated with silk sutures (3/0; Johnson & Johnson Medical Ltd) soaked in propylene glycol as the continuous loop on one side of the maxilla bone. Water in cages was supplemented with 5% high-sucrose drinking water for 4 weeks. Four weeks later, the ligation was removed and LMK-235 (S7569; Selleckchem) 20 mg/kg was administered via oral gavage for 4 weeks.

Micro computed tomography (μCT)

CEJ-ABC was analysed by rodent μCT (Rigaku Corporation). The imaging was performed at 90 kV and 200 mA for 3 minutes with a slice thickness of 50 μm. Two-dimensional (2D) images were acquired and analysed using TRI/3D-BON (Ratoc System Engineering Co., Ltd.).

Flow cytometry analysis

At the experimental end point, mice were sacrificed by CO_2 inhalation, and gingival tissues were collected (10 mice per group). Gingival tissues were dissected and dissociated by maceration and incubation with Trypsin-EDTA 0.25% (Thermo Fisher Scientific) and DNase and collagenase II for 40 minutes; the resulting cell suspension was washed with PBS and incubated with 2.5% bovine serum albumin (BSA) in PBS for 15 minutes and then with rat CD45 Alexa Flour 488 and CD11b APC for 30 minutes and washed with PBS. The negative population gate was set against cell suspension and incubated for 30 minutes with rat IgG2b kappa Alexa Flour 488 and Mouse IgG1 APC Isotype Control. The stained cell populations were recorded using the CyanADP flow cytometer

(Beckman Coulter), and the resulting 2D plots were analysed using FlowJo (FlowJo LLC).

Enzyme-linked immunosorbent assay (ELISA)

IL-1b assay kit (R&D Systems), IL-6 assay kit (R&D Systems), TNF-α assay kit (R&D Systems), and IL-23a assay kit (Abcam) were used according to the kit instructions. OD was detected using Synergy H1 (Biotek) recorded at 450 nm.

Western blot analysis

Western blot was performed as previously described.[17,18] Osteoclast cultures were washed with PBS and lysed by radioimmunoprecipitation assay buffer containing FAST protease inhibitors (Sigma-Aldrich). The protein concentration was quantified using Pierce BCA Protein Assay Kit (Thermo Fisher Scientific), and 30 μg of total protein per lane was separated by 4%–20% gradient sodium dodecyl sulfate–polyacrylamide gel. Separated proteins were transferred to 0.45-μm pore-size nitrocellulose membranes, with 30 to 50 μg total protein per lane. The membranes were blocked with 5% BSA (Sigma-Aldrich) at room temperature for 1 hour and then incubated overnight at 4 °C with the primary antibodies. After being washed with a PBS-Tween 20 buffer (Sigma-Aldrich), the blots were incubated with a horseradish peroxidase–conjugated secondary antibody (1:1000; Biorad) for 1 hour at room temperature. The signals were developed with enhanced chemiluminescence with a SuperSignal West Pico Kit (Thermo Fisher Scientific).

Plasmid transfection and immunoprecipitation

HEK293T (CRL-3216) cells were purchased from ATCC and grown in complete DMEM. HDAC5-flag plasmid (Addgene) and human influenza hemagglutinin (HA)-tagged p100 plasmid (Addgene) were transfected to mouse HEK293 cells using a lipofectamine 3000 transfection kit (Thermo Fisher Scientific). Briefly, 3 μL lipofectamine 3000 (100022052, Thermo Fisher Scientific) was diluted in 250 μL Opti-MEM Reduced Serum Medium (31985062; Thermo Fisher Scientific). The reagent P3000 (100022058; Thermo Fisher Scientific) was diluted in 250 μL Opti-MEM, and 1 μg of HDAC5-flag DNA was combined with reagent P3000. The solutions were gently mixed by inverting the tubes. After 10 minutes of incubation at room temperature, the mixture was added to HEK293T cells and incubated overnight. HEK cells were harvested for pull-down assays into Pierce TM IP Lysis buffer (87787; Thermo Fisher Scientific) supplemented containing FAST protease inhibitors (Cat#: S8830, Sigma-Aldrich). The 500 μg total protein was incubated with 2.5 μg of FLAG antibody or rabbit immunoglobulin G control at 4 °C overnight. Then immune complexes were conjugated with a 25-μL Protein A/G bead (Santa Cruz Biotechnology) for 2 hours. Proteins were eluted with RIPA buffer supplemented with β-Mercaptoethanol. The β-actin from total lysate was used as the loading control. For the whole osteoclast acetylation experiment, native p100 was pulled down by the p100 antibody from 500 μg of osteoclast cultures lysates by overnight incubation at 4 °C, and the acetylation level was determined by the acetylated-lysine antibody.

Statistical analysis

The statistical analysis and bar graph design were performed using GraphPad Prism software. The results are presented as mean ± SD. One-way analysis of variance (ANOVA) analysed multiple groups with Tukey multiple comparisons, and the 2 groups were compared with an unpaired *t* test (2-tailed). A *P* value <.05 was considered significant.

Results

Inhibition of HDAC4/5 by LMK-235 reduces osteoclast differentiation

To explore the regulatory mechanism of noncanonical NF-κB signaling in osteoclasts cells, we analysed the binding protein of p100 through STRING interaction network analysis (https://string-db.org/); we found that the p100 molecule can bind to multiple proteins, including HDAC4 and HDAC5 (Figure 1A). To verify the functions of the above molecules, we used the HDAC4/5 inhibitor LMK-235 to treat RANKL-induced primary osteoclast cultures. LMK-235 (10, 20 nM) significantly inhibited the osteoclast-specific genes *Acp5*, *Calcr*, and *Cstk* (Figure 1B) at mRNA levels. Furthermore, alkaline phosphatase activity, the main protein level indicator of osteoclastogenesis, was also significantly reduced by LMK-235 treatment in a dose-dependent manner (Figure 1C).

LMK-235 treatment ameliorates the experimental PD model in mice

Treatment with LMK-235 (20 mg/kg) for 4 weeks significantly reduced the cementoenamel junction–alveolar bone crest (CEJ-ABC) distance increase as analysed by μCT when compared with vehicle-treated controls (Figure 2A). Interestingly, NIK$^{-/-}$ mice with Map3k14 ablation and reduced noncanonical NF-κB activation did not experience significantly increased CEJ-ABC distance, nor were these mice significantly affected by LMK-235 treatment (Figure 2A). Flow cytometry analysis of dissociated gingival tissues in the chronic periodontis (CPD) model demonstrated substantial reduction of myeloid (CD45/CD11b) positive immune cell infiltration in LMK-235–treated mice (Figure 2B). Consistently, RT-PCR analysis of the mRNA extracted from gingival tissue of CPD mice similarly indicated a significant reduction of IL-1b, TNF-α, IL-6, and IL-23a transcription in LMK-235–treated mice (Figure 2C).

LMK-235 treatment reduces IL-23a expression in LPS- and Pam3csk4-mediated stimulation of primary osteoclast cultures in vitro

Primary osteoclast cultures were pretreated with LMK-235 and stimulated with LPS for 6 hours, inducing both canonical and noncanonical NF-κB activation. The mRNA levels of IL-1b, IL-6, TNF-α, and IL-23a were determined by RT-PCR

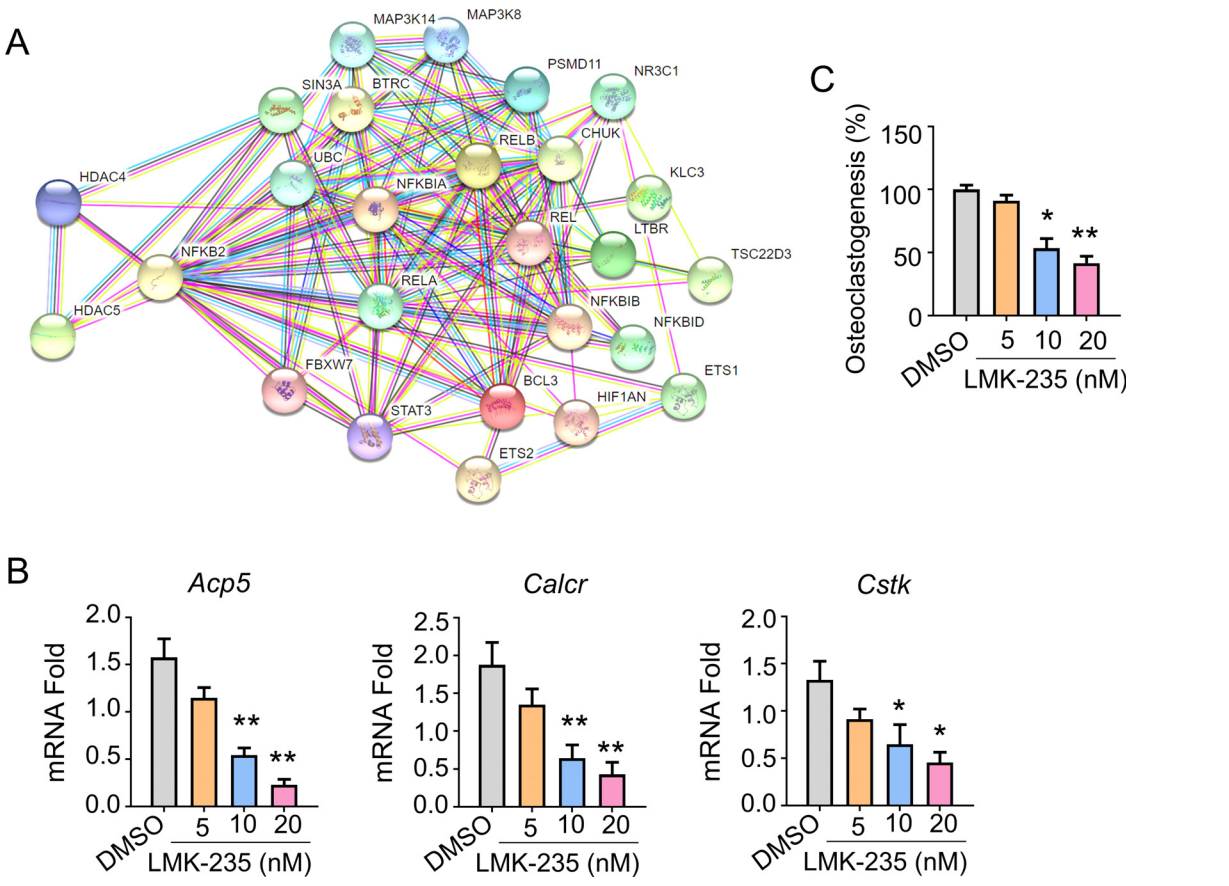

Fig. 1 – The HDAC5 inhibitor suppresses osteoclastogenesis. A, The interacted proteins of nuclear factor-κB2 (NF-κB2) were presented in the STRING interaction network. B, The expression of osteoclast marker genes *Cstk*, *Acp5*, and *Calcr* was determined by real-time polymerase chain reaction. C, Acid phosphatase activity in primary osteoclast cultures treated with LMK-235. Data are presented as mean ± SD values representing at least 3 independent experiments. Statistical analyses represent variations in experimental replicates. *P < .05. **P < .01. n = 8.

(Figure 3A). LMK-235 treatment did not affect the transcription of IL-1b, IL-6, or TNF-α but significantly reduced IL-23a gene levels. The mRNA-level data were further confirmed by ELISA detection of the respective protein expression following 24 hours of LPS stimulation, achieving the same results with only IL-23a being downregulated in LMK-235 (Figure 3B), but not other proinflammatory cytokines. Similar results were achieved when osteoclast cultures were pretreated with LMK-235 and then stimulated with the noncanonical NF-κB activator Pam3csk4 for 6 hours. Consistent with LPS results, only IL-23a was affected by the LMK-235 treatment (Figure 3C), but it did not affect the expression of other cytokines. These data indicate that LMK-235 predominately affects the noncanonical NF-κB activation pathway.

HDAC5 binds to p100, and its inhibition with LMK-235 increases p100 acylation, decreasing NF-κB activation

To study the effect of inhibiting HDAC5 on noncanonical NF-κB pathways, we pretreated primary cultured osteoclasts with LMK-235 at 20 nM before RANKL stimulation for 0, 12, and 24 hours. The NF-κB p52 subunit decreased in the nuclear fraction, indicating activation of the noncanonical NF-κB pathway with the inhibition of HDAC4/5 (Figure 4A). The interaction of HDAC5 with p100 was further confirmed by the overexpression of Flag-tagged HDAC5 and human influenza HA-tagged p100 in HEK293 cells following Flag antibody pull-down, and HA-p100 was strongly detected in the pull-down lanes HDAC5 (Figure 4B). The increase of acetylation levels of p100 was further confirmed by p100 antibody pull-down from primary osteoclast cultures and detection of the increase of acetylated-lysine in the pull-down lanes of LMK-235–treated cultures (Figure 4C).

NIK$^{-/-}$ mice demonstrate reduced osteoclast differentiation and are unaffected by LMK-235 treatment

Consistent with Figure 1C, primary bone marrow cultures isolated from WT animals demonstrated decreased osteoclast markers *Acp5*, *Clcr*, and *Cstk* mRNA levels when treated with LMK-235. However, bone marrow cultures isolated from NIK$^{-/-}$ mice indicated baseline decreases in mRNA levels of osteoclast markers, which were not significantly affected by LMK-235 treatment (Figure 4D), suggesting impaired NF-κB activation and osteoclast differentiation in NIK$^{-/-}$ mice.

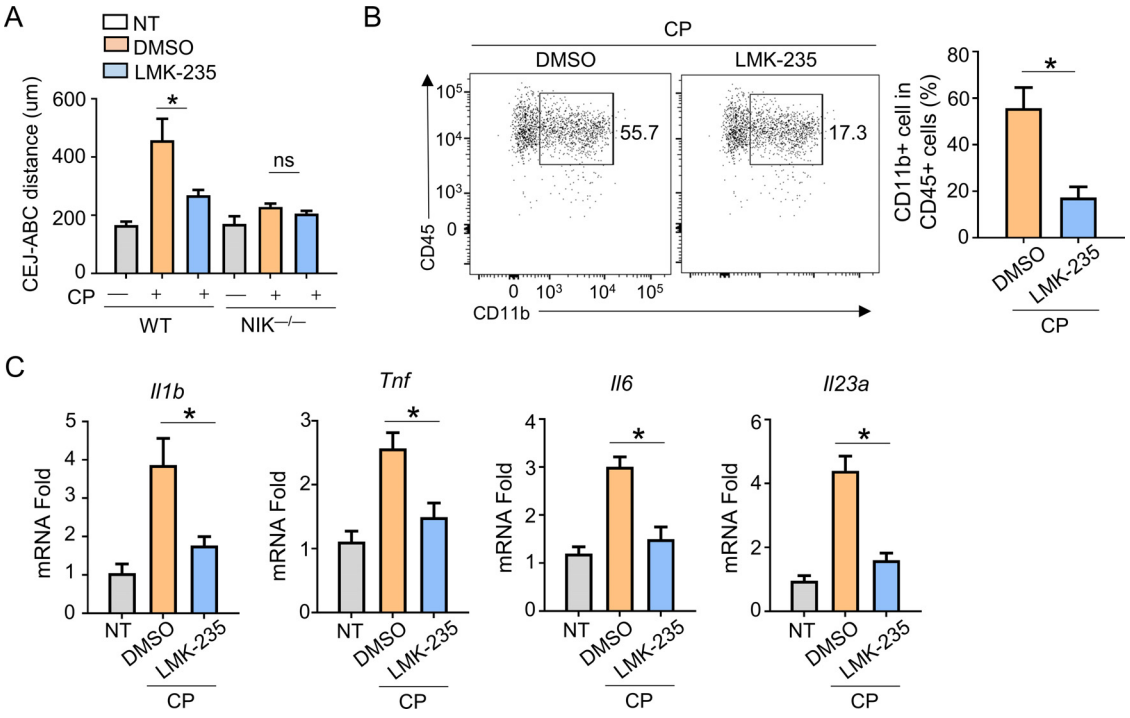

Fig. 2 – The HDAC5 inhibitor disrupts the onset of chronic periodontitis (CPD). A, The cementoenamel junction–alveolar bone crest was analysed via micro computed tomography in wild-type and NIK$^{-/-}$ mice in the CPD model treated with LMK-235 (20 mg/kg) or vehicle. Naÿve mice were used as controls. A one-way analysis of variance (ANOVA) with Tukey multiple comparisons was used to determine statistical significance. *P < .05. n = 10. B, The frequency of infiltrating myeloid cells CD45/CD11b positive in gingival tissues from the mice with CPD treated with vehicle or LMK-235 (20 mg/kg) was evaluated by flow cytometry analysis. Student t test was used to determine statistical significance. *P < .05. n = 10. C, The mRNA levels of interleukin (IL)-1β, tumor necrosis factor alpha, IL-6, and IL-23a in gingival tissues from mice with CPD treated with vehicle or LMK-235 (20 mg/kg) were evaluated by real-time polymerase chain reaction (n = 3 per group) with 3 technical replicates. All data are presented as fold change of the naÿve group. β-actin mRNA level is used as the housekeeping gene. Values are represented by 3 independent experiments with 3 technical replicates for each sample. A one-way ANOVA with Tukey multiple comparisons was used to determine statistical significance. *P < .05. n = 9.

Discussion

HDAC inhibition has been shown to reduce chronic inflammatory diseases,[19] including inhibition of the RANKL-RANK pathway.[20] HDACs are major gene expression regulators[21]; some HDAC members interact with transcription factors directly.[20] In the current study, we demonstrated that inhibition of HDAC5 by LMK-235 reduced osteoclast differentiation marker expression in vitro and ameliorated experimental CPD.

Increased RANK expression sensitised precursor cells for osteoclastic differentiation. NF-κB signaling participates in the regulation of osteoclast differentiation, activity, and survival.[11,22] The inhibitory protein IκB localises NF-κB in the cytoplasm until it is activated by dimerising with Rel family proteins, promoting nuclear translocation of the p52 subunit.[23] Noncanonical NF-κB signaling, however, leads to ubiquitination of p100, but instead of proteasomal degradation, p100 is processed to p52 and the resulting RelB:p52 heterodimers translocate to the nucleus.[24] In osteoclastogenesis expression, p52 levels increase within 2 hours after RANKL treatment and remain increased without changes in RelA or p50 mRNA levels.[25]

Our overexpression experiments in HEK293 cells definitively demonstrated the direct interaction of HDAC5 with the p100 subunit of the NF-κB pathway, and LMK-235 inhibition of HDAC5 results in an increase of p100 acetylation well as reduction of NF-κB p52 nuclear presence, presumably due to proteasomal degradation of acidulated p100, establishing deacetylation as the regulatory factor for noncanonical NF-κB activation. NIK$^{-/-}$ mice that lack p52 signaling indicate resistance to antigen-induced arthritis resulting from T cell responses.[26,27] Indeed, in our study, NIK-deficient mice did not indicate substantial PD development and were unaffected by LMK-235 treatment in vivo and primary osteoclast cultures, indicating that the NIK is part of the RANKL/RANK axis upstream of HDAC's regulation (Figure 5).

In CPD in vivo, we observed decreased expression of proinflammatory cytokines IL-1b, TNF-α, IL-6, and IL-23a in gingival tissues. However, in the primary osteoclast cultures, when stimulated by LPS which induces both canonical and noncanonical NF-κB[28] or Pam_3CSK_4 which only induces noncanonical NF-κB pathway activation,[29] only IL-23a expression was inhibited by LMK-235 treatment. Infiltrating monocytes and macrophages are the tissue's main sources of these

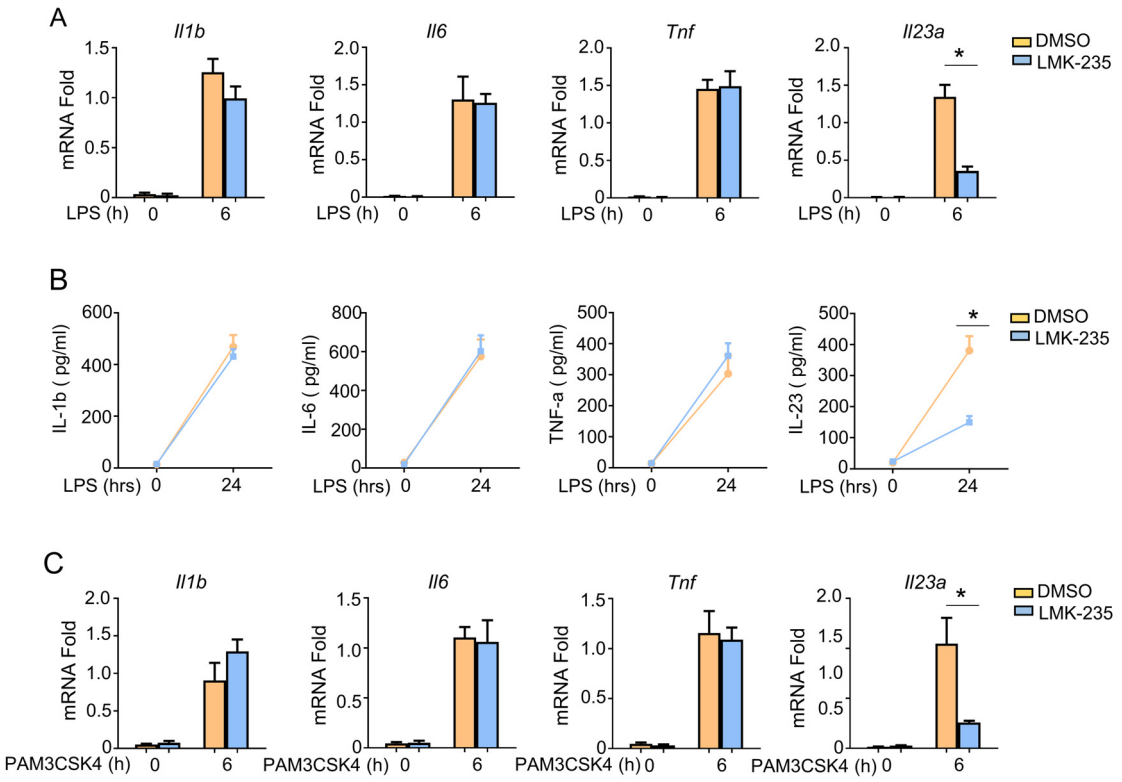

Fig. 3 – The HDAC5 inhibitor suppresses the production of interleukin (IL)-23. A, The mRNA levels of IL-1b, IL-6, tumor necrosis factor alpha (TNF-α), and IL-23a in primary osteoclast pretreated with LMK-235 (20 nM) or dimethyl sulfoxide (DMSO; 1 μL/mL) for 2 hours and stimulated with lipopolysaccharide (LPS) for 6 hours measured by real-time polymerase chain reaction (RT-PCR). B, Protein levels of IL-1b, IL-6, TNF-α, and IL-23a in the supernatants of osteoclast stimulated pretreated with LMK-235 (20 nM) or DMSO (1 μL/mL) for 2 hours and stimulated with LPS for 24 hours detected by enzyme-lined immunosorbent assay. C, IL-1b, IL-6, TNF-α, and IL-23a in primary osteoclast pretreated with LMK-235 (20 nM) or DMSO (1 μL/mL) for 2 hours and stimulated with PAM3CSK4 for 6 hours measured by RT-PCR. All data are presented as fold change of the naÿve group. β-actin mRNA level is used as a housekeeping gene. Values are represented by 3 independent experiments with 3 technical replicates for each sample. Student t test was used to determine statistical significance. *P < .05. n = 9.

inflammatory cytokines mediated by toll-like receptor (TLR) signaling.[30] In the osteoclast cultures, however, IL-23a is upregulating RANK expression and mediating osteoclast-like cells, indicating an IL-23a–mediated positive feedback loop in osteoclasts that in turn facilitates activation and recruitment of macrophages. These results may also suggest the more broad effect of LMK-235 in other cell types, including infiltrating macrophages in the gingival tissues.

Further studies include replicating the effects of LMK-235 in the human microflora inoculation model in rats and testing LMK-235 on the nonrodent model of PD.[31] On the molecular level, the combination of LMK-235 with TLR inhibitors may potentiate the effects of HDAC5 inhibition, as both arcs of NF-κB activation through colony stimulating factor receptor and TLR would be disrupted.[32] Investigation of the effects of cytokines through recombinant cytokines and macrophage condition media on LMK-235–treated osteoclasts, as well as the direct effect of LMK-235 on macrophages, would allow further understanding of the role of HDAC5 inhibition and p100 acetylation in the PD inflammatory process.

Currently, the treatment of PD is limited to surgical removal of the affected tissue, topical and oral antibiotic use, anti-inflammatory treatment, and enhanced oral hygiene.[33] None of the treatment protocols include direct modulation of bone resorption and osteoclast activity. Currently, several ongoing clinical trials already use HDAC inhibitors in human patients, predominantly in cancers such as multiple myeloma.[34] Whilst systemic application of LMK-235 for the treatment of PD may be undesirable due to potential side effects and systemic toxicity, the topical use in combination with antibiotic treatment or a small dose intraperiodontal pocket delivery[35] may mitigate the issue of systemic side effects, opening a new prospect for PD therapies that directly target osteoclast activity and inflammatory infiltration of the gum tissues.

Limitations

The LMK-235 inhibitor used in this study inhibits HDAC4 and 5. Our in vitro experiments have ascertained the functions of HDAC5 in noncanonical NF-κB activation. However, the HDAC4 contribution to the observed in vivo and in vitro results requires further study. Primary osteoclast cultures were validated by the expression of osteoclast-specific

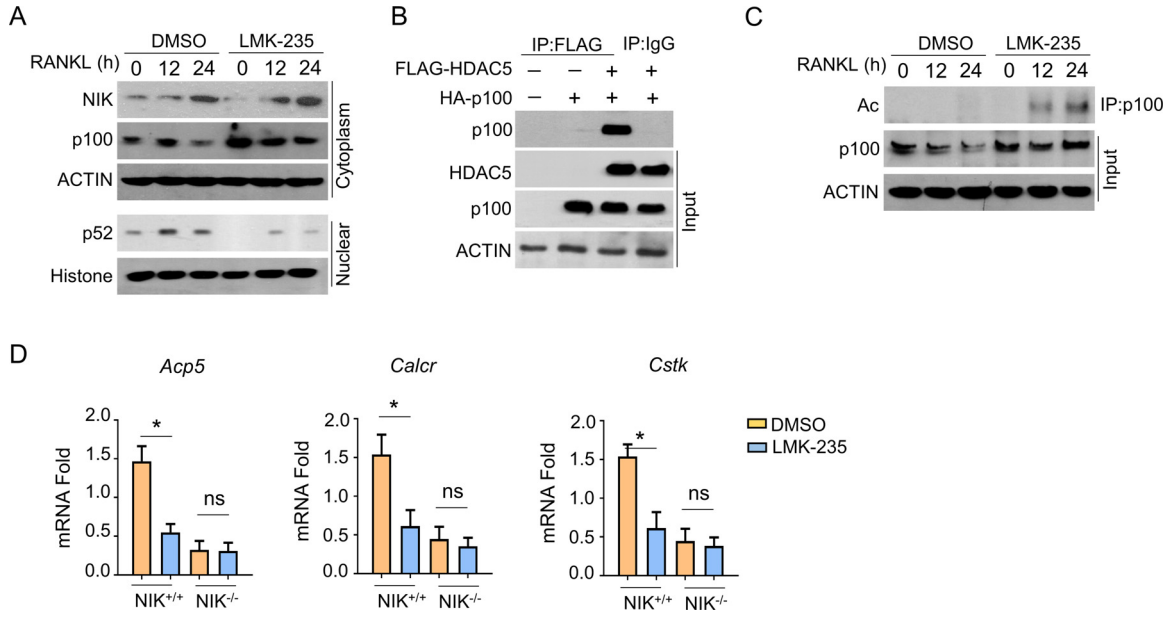

Fig. 4 – HDAC5 interacts with p100 and removes its acetylation. A, Western blot analysis of the nuclear factor-κB–inducing kinase, p100 in cytoplasmic and nuclear factor-κB p52 in the nuclear extracts isolated from primary bone marrow cultures following RANKL (0-, 12-, and 24-hour time points) induced differentiation to osteoclasts with and without LMK-235 (20 nM). The loading control in the cytoplasmic fraction was β-actin in the nuclear fraction histone H1. B, Detection of p100 in immunoprecipitation of flag-tagged HDAC5 in HEK293T cells transfected with HDAC-5-flag plasmid 24 hours after transfection. C, Immunoblot analysis of p100 acetylation by detecting acetylated-lysine in whole-cell lysates of osteoclast treated with LMK-235 (20 nM) for the indicated time points. D, The expressions of osteoclast genes *Acp5*, *Calcr*, and *Cstk* were determined by quantitative polymerase chain reaction. β-actin was used as the housekeeping gene. Student t test was used to determine statistical significance. *P < .05. n = 9.

markers *Acp5*, *Calcr*, and *Cstk* and TRAP activity. However, we can not fully exclude the possibility of the presence of a small population of the other cell types. The ligature-induced PD model is well established and accepted. However, it includes a substantial inflammatory component of the foreign body presence. The effect of HDAC5 inhibition on other animal

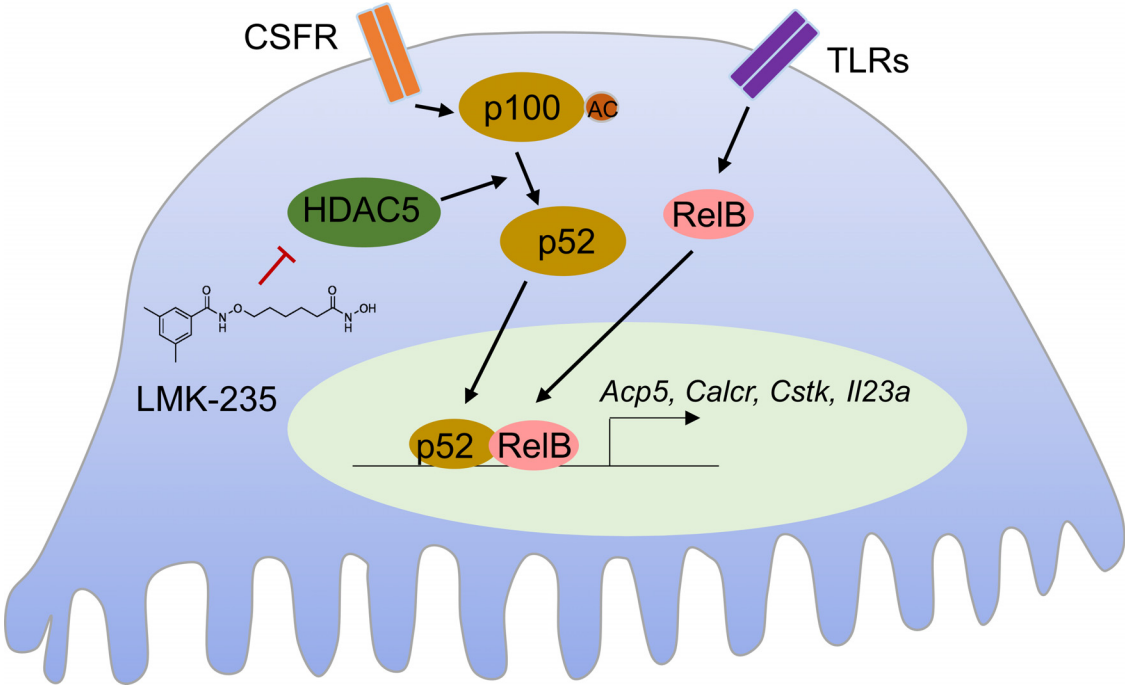

Fig. 5 – Schematic image illustrating the molecular mechanisms.

models of PD, such as microflora inoculation, warrants further investigation.

Conclusions

This work has identified HDAC5 as a direct regulator of NF-κB p100 subunit deacetylation which facilitates p52 noncanonical NF-κB activation as part of osteoclast-mediated bone resorption and PD development.

Conflict of interest

None disclosed.

REFERENCES

1. Kononen E, Gursoy M, Gursoy UK. Periodontitis: a multifaceted disease of tooth-supporting tissues. J Clin Med 2019;8(8):1135.
2. Paula-Silva FWG, Arnez MFM, de Campos Chaves Lamarque G, et al. Osteoclast formation, inflammation, and matrix metalloproteinase-9 are downregulated in bone repair following root canal treatment in dogs teeth. Clin Oral Investig 2021;25(7):4699–707.
3. Lang NP, Bartold PM. Periodontal health. J Periodontol 2018;89(Suppl 1):S9–16.
4. Kinney JS, Ramseier CA, Giannobile WV. Oral fluid-based biomarkers of alveolar bone loss in periodontitis. Ann N Y Acad Sci 2007;1098:230–51.
5. Roberts FA, Hockett Jr RD, Bucy RP, Michalek SM. Quantitative assessment of inflammatory cytokine gene expression in chronic adult periodontitis. Oral Microbiol Immunol 1997;12(6):336–44.
6. Hou L-T, Liu C-M, Liu B-Y, Lin S-J, Liao C-S, Rossomando EF. Interleukin-1β, clinical parameters and matched cellular-histopathologic changes of biopsied gingival tissue from periodontitis patients. J Periodontal Res 2003;38(3):247–54.
7. Chen B, Wu W, Sun W, Zhang Q, Yan F, Xiao Y. RANKL expression in periodontal disease: where does RANKL come from? Biomed Res Int 2014;2014:731039.
8. Sun SC. Non-canonical NF-kappaB signaling pathway. Cell Res 2011;21(1):71–85.
9. Liu T, Zhang L, Joo D, Sun S-C. NF-κB signaling in inflammation. Signal Transduct Target Ther 2017;2(1):17023.
10. Yu J-A, Jin J, Li Y-Y. The physiological functions of IKK-selective substrate identification and their critical roles in diseases. STEMedicine 2020;1(4):e49.
11. Boyce BF, Xiu Y, Li J, Xing L, Yao Z. NF-kappaB-mediated regulation of osteoclastogenesis. Endocrinol Metab (Seoul) 2015;30(1):35–44.
12. Wada T, Nakashima T, Hiroshi N, Penninger JM. RANKL-RANK signaling in osteoclastogenesis and bone disease. Trends Mol Med 2006;12(1):17–25.
13. Li G, Tian Y, Zhu WG. The roles of histone deacetylases and their inhibitors in cancer therapy. Front Cell Dev Biol 2020;8:576946.
14. Verbeek TCAI, Arentsen-Peters S, Garrido Castro P, et al. Selective inhibition of class II HDAC isoforms 4 and 5 provides a promising therapeutic intervention for MLL-rearranged acute lymphoblastic leukemia in infants. Blood 2021;138:2206.
15. Place RF, Noonan EJ, Giardina C. HDAC inhibition prevents NF-kappa B activation by suppressing proteasome activity: down-regulation of proteasome subunit expression stabilizes I kappa B alpha. Biochem Pharmacol 2005;70(3):394–406.
16. Lennikov A, Saddala MS, Mukwaya A, Tang S, Huang H. Autoimmune-mediated retinopathy in CXCR5-deficient mice as the result of age-related macular degeneration associated proteins accumulation. Front Immunol 2019;10:1903.
17. Huang H, Shen J, Vinores SA. Blockade of VEGFR1 and 2 suppresses pathological angiogenesis and vascular leakage in the eye. PLoS One 2011;6(6):e21411.
18. Huang H, Van de Veire S, Dalal M, et al. Reduced retinal neovascularization, vascular permeability, and apoptosis in ischemic retinopathy in the absence of prolyl hydroxylase-1 due to the prevention of hyperoxia-induced vascular obliteration. Invest Ophthalmol Vis Sci 2011;52(10):7565–73.
19. Halili MA, Andrews MR, Sweet MJ, Fairlie DP. Histone deacetylase inhibitors in inflammatory disease. Curr Top Med Chem 2009;9(3):309–19.
20. Nakamura T, Kukita T, Shobuike T, et al. Inhibition of histone deacetylase suppresses osteoclastogenesis and bone destruction by inducing IFN-beta production. J Immunol 2005;175(9):5809–16.
21. Haberland M, Montgomery RL, Olson EN. The many roles of histone deacetylases in development and physiology: implications for disease and therapy. Nat Rev Genet 2009;10(1):32–42.
22. Soysa NS, Alles N. NF-kappaB functions in osteoclasts. Biochem Biophys Res Commun 2009;378(1):1–5.
23. Sun SC. The non-canonical NF-kappaB pathway in immunity and inflammation. Nat Rev Immunol 2017;17(9):545–58.
24. Madge LA, May MJ. The NFkappaB paradox: RelB induces and inhibits gene expression. Cell Cycle 2011;10(1):6–7.
25. Yamashita T, Yao Z, Li F, et al. NF-kappaB p50 and p52 regulate receptor activator of NF-kappaB ligand (RANKL) and tumor necrosis factor-induced osteoclast precursor differentiation by activating c-Fos and NFATc1. J Biol Chem 2007;282(25):18245–53.
26. Aya K, Alhawagri M, Hagen-Stapleton A, Kitaura H, Kanagawa O, Novack DV. NF-(kappa)B-inducing kinase controls lymphocyte and osteoclast activities in inflammatory arthritis. J Clin Invest 2005;115(7):1848–54.
27. Yang C, McCoy K, Davis JL, et al. NIK stabilization in osteoclasts results in osteoporosis and enhanced inflammatory osteolysis. PLoS One 2010;5(11):e15383.
28. Bhattacharyya S, Borthakur A, Dudeja PK, Tobacman JK. Lipopolysaccharide-induced activation of NF-kappaB non-canonical pathway requires BCL10 serine 138 and NIK phosphorylations. Exp Cell Res 2010;316(19):3317–27.
29. Funderburg NT, Jadlowsky JK, Lederman MM, Feng Z, Weinberg A, Sieg SF. The toll-like receptor 1/2 agonists Pam(3) CSK (4) and human beta-defensin-3 differentially induce interleukin-10 and nuclear factor-kappaB signalling patterns in human monocytes. Immunology 2011;134(2):151–60.
30. Papadopoulos G, Weinberg EO, Massari P, et al. Macrophage-specific TLR2 signaling mediates pathogen-induced TNF-dependent inflammatory oral bone loss. J Immunol 2013;190(3):1148–57.
31. Oz HS, Puleo DA. Animal models for periodontal disease. J Biomed Biotechnol 2011;2011:754857.
32. Gao W, Xiong Y, Li Q, Yang H. Inhibition of toll-like receptor signaling as a promising therapy for inflammatory diseases: a journey from molecular to nano therapeutics. Front Physiol 2017;8:508.
33. Jain N, Jain GK, Javed S, et al. Recent approaches for the treatment of periodontitis. Drug Discov Today 2008;13(21–22):932–43.
34. Ohguchi H, Hideshima T, Anderson KC. The biological significance of histone modifiers in multiple myeloma: clinical applications. Blood Cancer J 2018;8(9):83.
35. Nair SC, Anoop KR. Intraperiodontal pocket: an ideal route for local antimicrobial drug delivery. J Adv Pharm Technol Res 2012;3(1):9–15.